



# On efficiency and accuracy of sparse identification of bistable nonlinear energy sink chains

Qinghua Liu<sup>1</sup> · Qiyu Li<sup>1</sup> · Dong Jiang<sup>1</sup>

Received: 1 May 2024 / Revised: 24 June 2024 / Accepted: 27 June 2024

© The Author(s), under exclusive licence to Springer-Verlag GmbH Germany, part of Springer Nature 2024

## Abstract

Bistable nonlinear energy sinks have been widely studied in energy harvesting and vibration absorption systems. The precise identification of local bistable nonlinear stiffness force is of significance to predicting and controlling the dynamic responses. Sparse identification is a very popular data-driven method that has been widely used in nonlinear dynamics identification. However, the accuracy and efficiency of sparse identification of multi-degree-of-freedom bistable systems are still not yet investigated. Besides, the significance of physical information of basis functions in sparse identification has not been numerically validated. This paper established the model of Bistable Nonlinear Energy Sink Chains (BENSC) and the vibration absorption characteristic is numerically analyzed. The Sparse Identification of Nonlinear Dynamics Systems (SINDy) and physics-informed SINDy are conducted on two-degree-of-freedom to ten-degree-of-freedom BENSC systems. The results show that with the increase in noise levels, the identification accuracy will be greatly decreased using SINDy with third-order polynomial basis functions. Besides, the computing time is exponentially increased when the number of degrees of freedom increases. However, the physics-informed sparse identification with basis functions a priori still keeps an accuracy of around 0.5% even under the noise level of 20 dB. The identification efficiency greatly improved compared with SINDy using third-order polynomial basis functions. The results give new insights into the accuracy and efficiency issues of sparse identification applied to BENSC systems under noise.

**Keywords** Bistable nonlinear energy sinks · Nonlinear stiffness force · Physics-informed SINDy · Efficiency and accuracy

## 1 Introduction

In the past decade, bistable nonlinear energy sinks have received growing attention due to their wide applications in the fields of energy harvesting and vibration absorption [1, 2]. There are various types of bistable nonlinear energy sinks have been developed, e.g., well-designed bistable tracks [3], local bistable beams [4] and oblique springs integration [5]. The precise identification of local bistable nonlinear stiffness force plays an important role in designing and predicting the performance of vibration absorbers. However, the introduction of bistability poses a huge challenge to the identification of nonlinear stiffness forces in practical applications because of snap-through chaotic motions [6]. Many data-driven identification methods have been developed for

parameter identification of structural dynamics. However, balancing the efficiency and accuracy of identification will be a difficulty when it comes to high-degrees-of-freedom systems.

For nonlinear restoring force identification of single-degree-of-freedom bistable vibrating oscillators, many approaches have been developed to address this issue. Liu et al. comparatively studied the displacement and acceleration measurement restoring force surface method to identify nonlinear bistable nonlinear stiffness force and linear damping force [7]. Feldman proposed the Hilbert Vibration Decomposition (HVD) combined with the “FREEVIB” algorithm for the identification of the nonlinear stiffness force of the Duffing-Holmes bistable oscillator [8, 9]. Anastasio combined restoring force surface and nonlinear subspace methods to identify the nonlinear stiffness force of an asymmetric double-well Duffing oscillator and its nonlinear damping characteristics [10, 11]. Liu et al. [12] developed a two-stage nonlinear subspace method to identify the parameters of the nonlinear bistable piezoelectric energy harvester.

✉ Qinghua Liu  
liuqinghua@njfu.edu.cn

<sup>1</sup> School of Mechanical and Electronic Engineering, Nanjing Forestry University, Nanjing, China

Zhu et al. [13] integrated the Bayesian probability method to select the best model in nonlinear subspace identification which can improve the model reliability and accuracy of bistable nonlinear identification.

For nonlinear stiffness force identification in nonlinear energy sink structures, Wang et al. [14] employed the restoring force surface method to identify the nonlinear stiffness and damping of a piecewise linear nonlinear energy sink and a hyperbolic tangent function is used for characterization. Lund et al. [15] adopted an unscented Kalman filter to identify geometrically nonlinear stiffness and Coulomb damping in a nonlinear energy sink device. Moore developed the characteristic nonlinear system identification method which is based on Hilbert transform and analytical approach to identify the dynamics of local piecewise linear attachments [16]. These methods have typically been found to be accurate and reliable for their designed nonlinear energy sinks.

Recently, with the rapid development of the data-driven regression method, sparse identification using the SINDy algorithm has become a hot topic due to its robustness. Brunton et al. originally proposed the nonlinear dynamic equation discovery method based on sparse regression and applied it to Lorenz and Navier Stokes's equations [17]. Then, it has been developed in the multi-degree-of-freedom system with local polynomial and hysteretic nonlinear systems [18, 19]. The reason is it has high efficiency and strong anti-noise ability if proper basis function and numerical differentiation techniques are used [20]. However, compared with the traditional signal processing method, the selection of basis functions is unclear. If the assumed candidate model basis functions are inappropriate, the computing time will greatly increase and the accuracy will be influenced. As we all know, the iden-

tification time is very important in control. Therefore, it is necessary to investigate the accuracy and efficiency of sparse identification of high degrees of freedom nonlinear systems.

This paper proposed the concept of BNESC which is a strongly nonlinear multi-degree-of-freedom system with many local bistable attachments. The dynamic model and sparse identification using SINDy and the physics-informed SINDy method are presented. The numerical simulations of a two-degree-of-freedom and eight-degree-of-freedom BNESC will show the vibration suspension ability. Besides, the accuracy and efficiency of SINDy identification and physics-informed SINDy identification of BNESC will be illustrated on two to ten-degree-of-freedom BNESC under noise levels of 40 dB, 30 dB and 20 dB. Finally, some discussions are given.

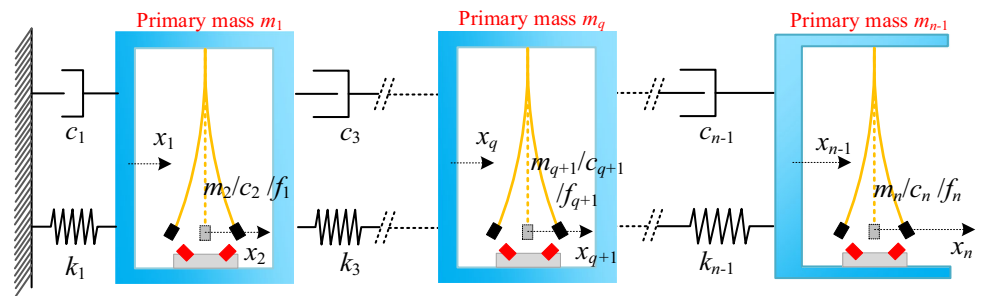
## 2 Modeling of BNESC

The system of Bistable Nonlinear Energy Sink Chains (BNESC) considered in this paper is schematically depicted in Fig. 1. It consists of  $n/2$  linear primary structures with  $n/2$  bistable nonlinear beams, where  $n$  represents the total degrees of freedom along the  $x$ -direction and also must be an even number. Every primary structure is connected to each other by a linear spring and linear damper. Besides, every primary structure has a bistable attachment with a linear damper and nonlinear magnetic coupled nonlinear stiffness force. When the BNESC is under impact or based excitation, the bistable nonlinear attachment will pump lots of energy from the primary mass and suppress the vibration of the main oscillator. Besides, the nonlinear bistable attachment can be used for energy harvesting.

The equations of motion of BNESC can be modeled as:

$$\left\{ \begin{array}{l} m_1 \ddot{x}_1 + c_1 \dot{x}_1 + k_1 x_1 + c_2 (\dot{x}_1 - \dot{x}_2) + \alpha_1 (x_1 - x_2) + \beta_1 (x_1 - x_2)^3 \\ \quad + c_3 (\dot{x}_1 - \dot{x}_3) + k_3 (x_1 - x_3) = 0 \\ m_2 \ddot{x}_2 + c_2 (\dot{x}_2 - \dot{x}_1) + \alpha_1 (x_2 - x_1) + \beta_1 (x_2 - x_1)^3 = 0 \\ \quad \ddots \\ m_q \ddot{x}_q + c_{q-1} (\dot{x}_q - \dot{x}_{q-2}) + k_{q-1} (x_q - x_{q-2}) + c_{q+1} (\dot{x}_q - \dot{x}_{q+1}) \\ \quad + \alpha_q (x_q - x_{q+1}) + \beta_q (x_q - x_{q+1})^3 + c_q (\dot{x}_q - \dot{x}_{q+2}) + k_q (x_q - x_{q+2}) = 0 \\ m_{q+1} \ddot{x}_{q+1} + c_{q+1} (\dot{x}_{q+1} - \dot{x}_q) + \alpha_q (x_{q+1} - x_q) + \beta_q (x_{q+1} - x_q)^3 = 0 \\ \quad \ddots \\ m_{n-1} \ddot{x}_{n-1} + c_{n-1} (\dot{x}_{n-1} - \dot{x}_{n-3}) + k_{n-1} (x_{n-1} - x_{n-3}) + c_n (\dot{x}_{n-1} - \dot{x}_n) \\ \quad + \alpha_{n-1} (x_{n-1} - x_n) + \beta_{n-1} (x_{n-1} - x_n)^3 = 0 \\ m_n \ddot{x}_n + c_n (\dot{x}_n - \dot{x}_{n-1}) + \alpha_{n-1} (x_n - x_{n-1}) + \beta_{n-1} (x_n - x_{n-1})^3 = 0 \end{array} \right. \quad (1)$$

**Fig. 1** Schematic view of BNESC system



where  $m$  is the equivalent mass of each primary structure and bistable nonlinear attachment.  $x$  is the displacement response of each oscillator. The subscript  $n$  represents where the mass is. The linear stiffness and damping are represented by  $k$  and  $c$ . The bistable nonlinear stiffness forces are all assumed third-order polynomials with coefficients of  $\alpha, \beta$  with different subscripts.

### 3 SINDy and physics-informed SINDy of BNESC

When the BNESC is described by Eq. (1), the linear parameters of  $m, k,$  and  $c$  can be easily measured or identified by linear parameter identification methods. However, the bistable nonlinear stiffness force is always hard to measure or identify due to snap-through characteristics. Besides, the bistable nonlinear stiffness force is strongly sensitive to the installation parameters of two rotatable magnets.

For modern data-driven methods, the sparse identification of nonlinear dynamical systems has the following procedures [17, 21]. Firstly, Eq. (1) is rewritten as the following forms:

$$\frac{dy_k(t)}{dt} = \Theta(y)\xi_k + \sigma Z_k \tag{2}$$

where  $\Theta(y)$  is the candidate function and  $\xi_k$  contains the coefficients of the sparse vector. The  $\sigma$  here is defined as the Signal to Noise Ratio (SNR) and  $Z_k$  is the root mean square of the measured data  $y_k(t)$ .

It must be noted that numerical differentiation techniques and robust noise removal methods in Eq. (2) may play an important role in SINDy identification accuracy [22–24]. In this paper, these advanced techniques will not be compared in detail.

According to Eq. (2), the candidate function  $\Theta(y)$  consists of polynomial terms, therefore:

$$\Theta(\mathbf{Y}) = \left[ \theta_1(\mathbf{Y}) \ \theta_2(\mathbf{Y}) \ \cdots \ \theta_P(\mathbf{Y}) \right] = \begin{bmatrix} \vdots & \vdots & \vdots & \vdots \\ \mathbf{Y}^{P_1} & \mathbf{Y}^{P_2} & \cdots & \mathbf{Y}^{P_n} \\ \vdots & \vdots & \vdots & \vdots \end{bmatrix} \tag{3}$$

where  $\mathbf{Y}^{P_n}$  denotes the  $n$ -order polynomial nonlinearities in the state space  $\mathbf{Y}$ .

To explain the importance of candidate function  $\Theta(y)$  selection in SINDy, a two-degree-of-freedom BNESC is taken as an example:

$$\begin{aligned} m_1 \ddot{x}_1 + c_1(\dot{x}_1 - \dot{x}_2) + k_1(x_1 - x_2) + c_2(\dot{x}_1 - \dot{x}_2) \\ + \alpha(x_1 - x_2) + \beta(x_1 - x_2)^3 = 0 \\ m_2 \ddot{x}_2 + c_2(\dot{x}_2 - \dot{x}_1) + \alpha(x_2 - x_1) + \beta(x_2 - x_1)^3 = 0 \end{aligned} \tag{4}$$

Derive the first-order differential equation by reducing the order in Eq. (4):

$$\begin{cases} dy(1) = y(2) \\ dy(2) = -\frac{c_1+c_2}{m_1}[y(2) - y(4)] \\ \quad -\frac{k_1+\alpha}{m_1}[y(1) - y(3)] - \frac{\beta}{m_1}[y(1) - y(3)]^3 \\ dy(3) = y(4) \\ dy(4) = -\frac{c_2}{m_2}[y(4) - y(2)] - \frac{\alpha}{m_2}[y(3) - y(1)] \\ \quad -\frac{\beta}{m_2}[y(3) - y(1)]^3 \end{cases} \tag{5}$$

where  $y(1)$  is equal to  $x_1$  and  $y(3)$  is equal to  $x_2$ .

Based on Eq. (5), the basis function only has basis function terms of

$$\Theta_{\text{prior}} = \left\{ y(2) \ y(2) - y(4) \ y(1) - y(2) \ [y(1) - y(3)]^3 \ y(4) \ y(4) - y(2) \ y(3) - y(1) \ [y(3) - y(1)]^3 \right\} \tag{6}$$

where  $\Theta_{\text{prior}}$  represents physics-informed basis functions.

There are only 8 terms of basis functions in Eq. (6). However, the basis functions will contain 35 terms if a third-order polynomial is chosen for identification in SINDy. The nonlinear basis functions will greatly be increased with the increase in degrees of freedom or polynomial order. The identification efficiency will greatly decrease if the basis functions in Eq. (3) are not physically informed.

**Table 1** Illustration of parameters of BNESC

BNESC	Two-degree-of-freedom	Eight-degree-of-freedom
Primary mass	$m_1 = 1 \text{ kg}$	$m_1 = m_3 = m_5 = m_7 = 1 \text{ kg}$
NES mass	$m_2 = 0.01 \text{ kg}$	$m_2 = m_4 = m_6 = m_8 = 0.01 \text{ kg}$
Primary damping	$c_1 = 1 \text{ N/(m/s)}$	$c_1 = c_3 = c_5 = c_7 = 1 \text{ N/(m/s)}$
NES damping	$c_2 = 0.02 \text{ N/(m/s)}$	$c_2 = c_4 = c_6 = c_8 = 0.02 \text{ N/(m/s)}$
Linear stiffness	$k_1 = 30,000 \text{ N/m}$	$k_1 = k_3 = k_5 = k_7 = 30,000 \text{ N/m}$
Nonlinear stiffness	$\alpha = -100 \text{ N/m}$ and $\beta = 10^6 \text{ N/m}^3$	

Once the basis function is established, the coefficients  $\xi$  can be obtained by performing a standard regression. The  $L^1$  regularization term needs to be added to the regression:

$$\xi = \underset{\xi'}{\operatorname{argmin}} \|\Theta \xi' - \mathbf{y}\|_2 + \lambda \|\xi'\|_1 \quad (7)$$

where  $\lambda$  weights the sparsity constraint. The formula is related to compressed sensing, which allows sparse vectors to be determined from relatively few noncoherent random measurements [25].

The specific identification processes of SINDy and physics-informed SINDy for BNESC can be summarized as follows:

1. Give the BNESC an impact or initial displacement at any degree of freedom;
2. Collect the displacement responses of each-degree-of-freedom;
3. Obtain the velocity and acceleration by numerical differentiation;

4. Rearrange matrices of displacement, velocity and acceleration signals based on Eqs. (5) and (6);
5. Select an appropriate polynomial order based on Eqs. (3) or (6) of nonlinear stiffness force and then construct the candidate function matrix in sparse regression;
6. Use the sequential thresholded least-squares algorithm to achieve sparse regression and the coefficients  $\xi$  can be identified.
7. Select the identified parameters and then reconstruct the nonlinear stiffness for comparison.

## 4 Numerical analysis of vibration absorption

To give specific views of vibration suppression abilities of BNESC systems. Two numerical simulations on two-degree-of-freedom BNESC and eight-degree-of-freedom BNESC are illustrated. According to current studies of bistable nonlinear energy sink analysis, third-order polynomial functions are adopted for nonlinear stiffness force characterization [26–31]. In the following simulations, the four nonlinear bistable beams all have the same nonlinear stiffness force with a function of  $f = -100x + 10^6x^3$ . The selected parameters in Eq. (1) are all illustrated in Table 1.

For two-degree-of-freedom BNESC, the initial condition of Eq. (1) is set as  $[0; 1 \text{ m/s}; 0; 0]$ . The sampling frequency of 1000 Hz in the time interval of  $t = 0$  to  $t = 6 \text{ s}$  is set. The displacement responses of mass  $m_1$  and  $m_2$  are obtained by conducting a Runge–Kutta ode45 simulation. Figure 2 shows the displacement responses of  $m_1$  and  $m_2$ . It can be observed that the nonlinear energy sink mass moves across two potential wells in the first 2.5 s and finally moves into the positive equilibrium point of  $+0.01 \text{ m}$ . The primary structure's vibration is suppressed and the amplitude quickly decays to zero.

To give a specific view of vibration suppression ability, the dynamic response of the primary mass of BNESC is

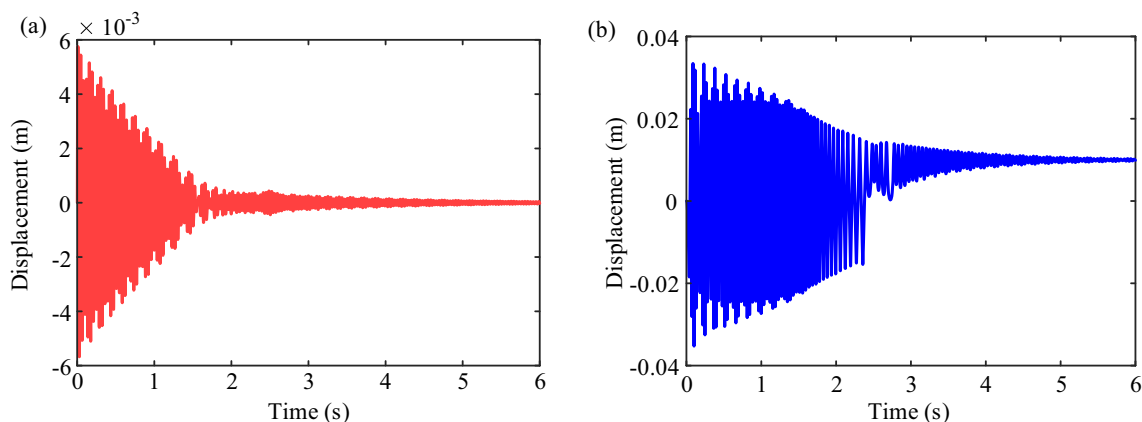


**Fig. 2** The dynamic responses of two-degree-of-freedom BNESC. **a** primary mass response. **b** nonlinear energy sink mass response

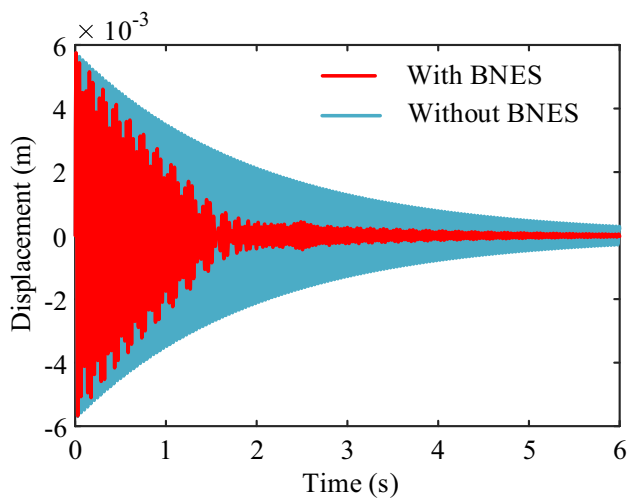


**Fig. 3** Comparison of free vibration responses of primary structure with BNES and without BNES

compared with no BNES primary structure, as shown in Fig. 3. The dynamic response of the primary structure without BENS is exponentially descending. However, the free

attenuation response with BNES has faster attenuation and smaller amplitude characteristics.

For eight-degree-of-freedom BNESC, the initial condition of Eq. (1) is set as  $[0; 3 \text{ m/s}; 0; 0; 0; 0; 0; 0; 0; 0; 0; 0; 0; 0; 0]$ . The sampling frequency of 1000 Hz in the time interval of  $t = 0$  to  $t = 6 \text{ s}$  is set. The displacement responses of mass  $m_1$  to  $m_8$  are obtained by conducting a Runge–Kutta ode45 simulation. Figure 4 shows the displacement responses of  $m_1$  to  $m_8$ . It can be observed that four BNES masses move across two potential energy wells at the beginning and then fall into any two equilibrium points. The primary structures of  $m_1, m_3, m_5$  and  $m_7$  exhibit irregular attenuation.

Figure 5 shows the nonlinear vibration suppression ability of eight-degree-of-freedom BNESC. The amplitude of the primary structure in BENS is always lower than the linear four-degree-of-freedom system without BNES. It must be noted that the BNESC is not optimized in this paper. Therefore, the vibration absorption is not as good enough. The optimization and design of a bistable nonlinear energy sink structure can refer to these references [32–34]. It must be noted that the selection of parameters in BNESC will not

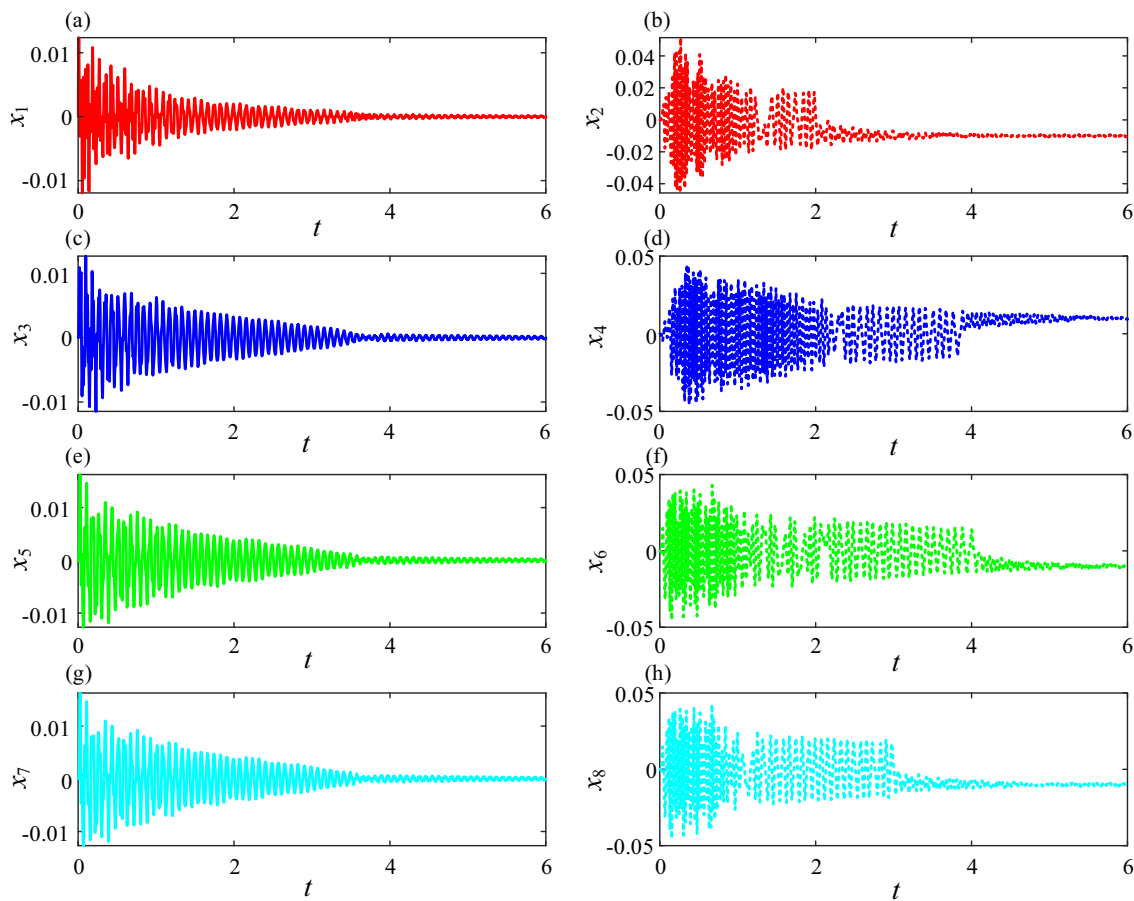


**Fig. 4** Free vibration responses of eight-degree-of-freedom BNESC

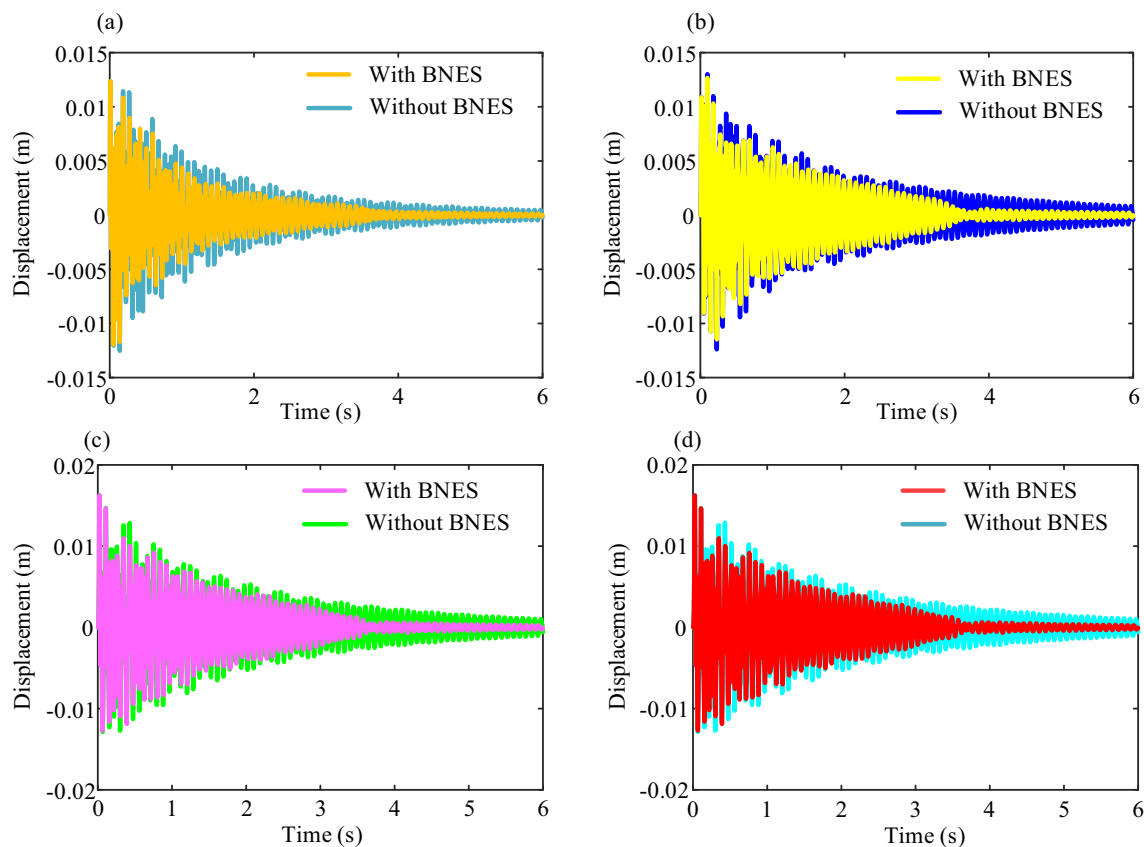


**Fig. 5** Comparison of vibration suppression ability with and without BNES

affect the identification results due to that third-order polynomial function was used to represent nonlinear stiffness force of BNESC. Theoretically, the identification procedure will not be affected if basis functions, noise interference and sparse regression algorithm were determined, as described in Eqs. (2), (3) and (7).

## 5 Identification accuracy and efficiency of BNESC

The dynamic responses of a BNESC are sensitive to nonlinear stiffness force parameters and initial conditions due to the strongly nonlinear coupling characteristics. Therefore, the Normalized Mean Square Error (NMSE) of the nonlinear stiffness force is defined here to evaluate identification accuracy.

$$J = \frac{100}{N\sigma_f^2} \sum_{i=1}^N (f - \hat{f}_i)^2 \quad (8)$$

where  $N$  denotes the total sampling points of nonlinear stiffness force. The  $\sigma_f^2$  is the variance of theoretical nonlinear

stiffness force. The  $\hat{f}$  is the identified nonlinear stiffness force sequence.

The sparse identification algorithm is conducted on two-degree-of-freedom to ten-degree-of-freedom systems. Besides, the 40 dB, 30 dB and 20 dB Gaussian White Noise are added to the displacement responses of each degree of freedom. Figure 6a shows the comparison between the identified nonlinear stiffness force and theory. It has a good agreement with the theory even under the noise level of 20 dB. Besides, it can be seen in Fig. 6b that with the increase in noise levels, the relative error between identified and theory greatly increased.

For eight-degree-of-freedom BNESC, the identified nonlinear stiffness force has a good agreement with the theory when the noise level is under 30 dB, as shown in Fig. 7a. There is an unreasonable error if the noise level increases to 20 dB. Figure 7b gives a comparison of identified relative errors under different noise levels. It demonstrates that with the increase in noise levels, a sharp increase in identification NMSE.

Table 2 lists the identified NMSE error from two to ten-degree-of-freedom BNESC. With the increase in the degrees of freedom, the identified nonlinear stiffness force error is increased. The same is true for the influence of noise levels

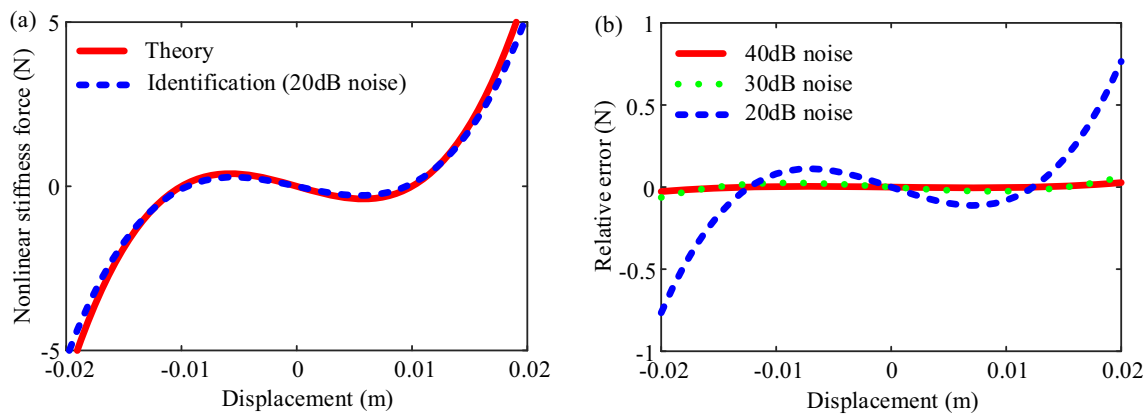


**Fig. 6** Identified nonlinear stiffness force and relative error of a two-degree-of-freedom BNESC. **a** comparison between the identified (20 dB) and theory. **b** relative error

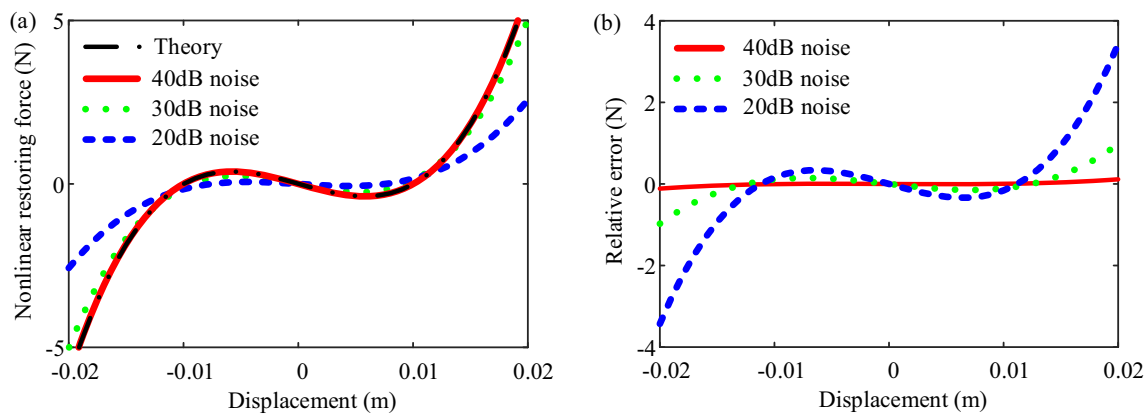


**Fig. 7** Identified nonlinear stiffness force and relative error of an eight-degree-of-freedom BNESC. **a** comparison between the identified (40 dB, 30 dB, 20 dB) and theory. **b** relative error

**Table 2** Identification results of BNESC under different noise levels

Noise levels (dB)	Degrees of freedom				
	Two (%)	Four (%)	Six (%)	Eight (%)	Ten (%)
40	0.0018	0.0027	0.0039	0.0358	0.6450
30	0.0331	0.1128	0.4716	2.3555	9.7115
20	2.1564	5.8351	9.0256	30.3485	63.0856

on the accuracy of nonlinear stiffness force identification. Under the noise level of 20 dB, the identified results in eight and ten-degree-of-freedom BNESC are 30.3485% and 63.0856%, respectively. The results demonstrate that if the noise level and degrees of freedom are simultaneously very high, the sparse identification may fail to identify the nonlinear stiffness force. However, under the noise level of 40 dB, the identified nonlinear stiffness has good accuracy with the highest NMSE of only 0.6450%. Even under the noise level of 30 dB, the identified results are also relatively good with NMSE of 0.0331% to 9.7115%.

To give a specific view of identification accuracy and efficiency of sparse identification with third-order polynomial basis functions for BNESC, 100 cycles on BNESC systems with different degrees of freedom are performed. Figure 8a–c show the relationship between NMSE and degrees of freedom under noise levels of 40 dB, 30 dB and 20 dB, respectively. The noise levels and degrees of freedom all have a great impact on identification accuracy. Figure 8d gives the relationship between computing time and degrees of freedom. It can be observed that the identification efficiency is greatly decreased with the increase in degrees of freedom.

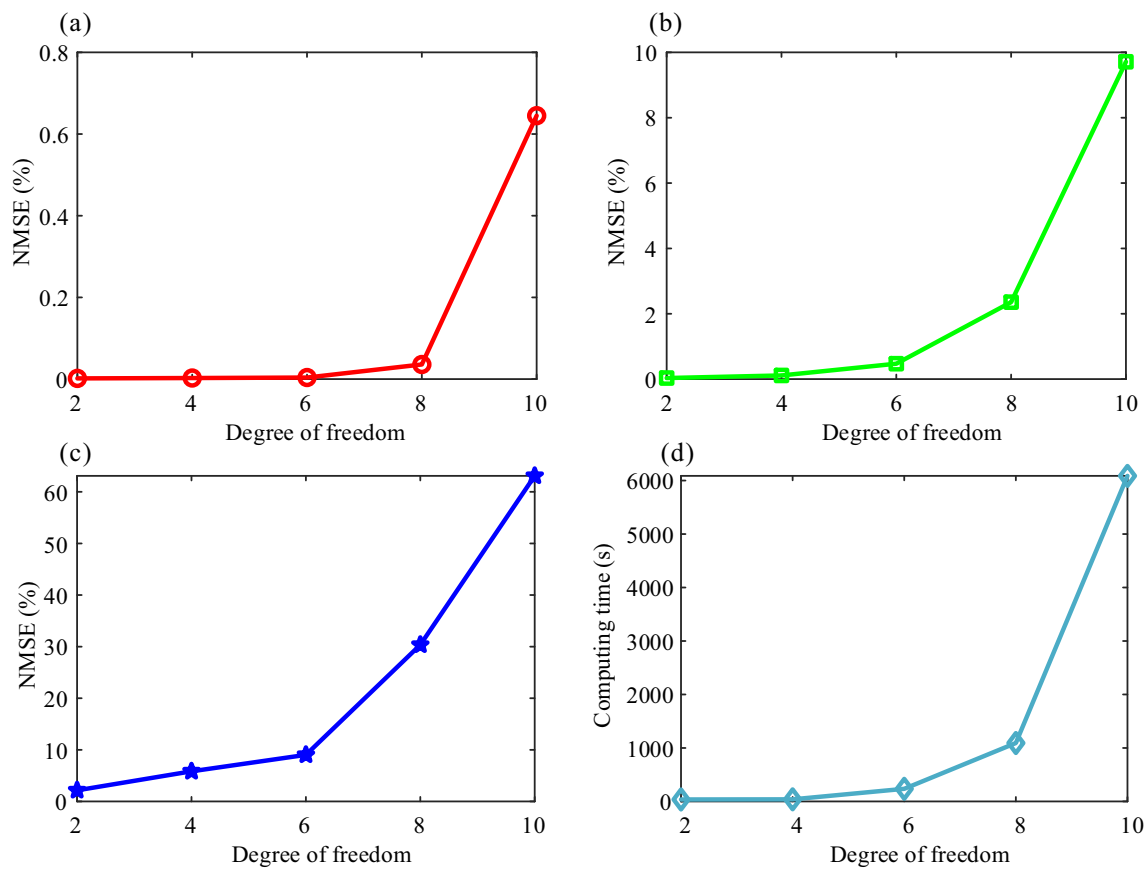


**Fig. 8** Identification accuracy and computing time using the SINDy method with a third-order polynomial. **a** Identification accuracy versus degrees of freedom (40 dB). **b** Identification accuracy versus degrees of freedom (30 dB). **c** Identification accuracy versus degrees of freedom (20 dB). **d** the computing time versus degrees of freedom (20 dB).

freedom (30 dB). **c** Identification accuracy versus degrees of freedom (20 dB). **d** the computing time versus degrees of freedom (20 dB).

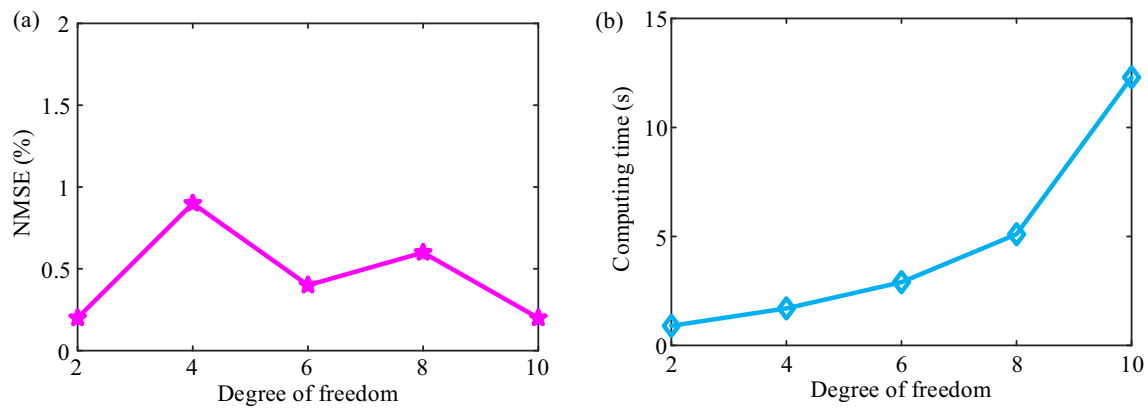


**Fig. 9** Identification accuracy and computing time using physics-informed SINDy. **a** Identification accuracy versus degrees of freedom (20 dB). **b** computing time versus degrees of freedom (20 dB)



To give a comparison, 100 cycles using physics-informed SINDy on a BNESC system with different degrees of freedom are performed. The identified accuracy keeps around 0.5% even under the noise of 20 dB, as depicted in Fig. 9a. Besides, the computing times are 0.9 s, 1.7 s, 2.9 s, 5.1 s and 12.3 s for two degrees of freedom to ten degrees of freedom BNESC, respectively. The identification accuracy greatly improved compared to SINDy identification with third-order polynomial basis functions, as shown in Fig. 9b.

## 6 Conclusions

This paper gives a new investigation on the efficiency and accuracy of sparse identification and physics-informed sparse identification of bistable nonlinear energy sink chains (BNESC). The numerical simulations of a two-degree-of-freedom and eight-degree-of-freedom BNESC have shown the vibration suppression ability. The relationship between the identified NMSE of nonlinear stiffness force and degrees of freedom of BNESC is illustrated. Besides, the 40 dB, 30 dB and 20 dB noise are added to test the anti-noise robustness. With the increase in degrees of freedom and noise levels, the identification accuracy will be greatly decreased using SINDy with third-order polynomial functions. However, the identification accuracy remains around 0.5% if the prior basis function of BNESC is known. Besides, the identification efficiency will greatly improve compared with SINDy. The investigated results give special views of the significance of basis function information for the identification of BNESC system. However, the acquisition of prior information of basis functions in SINDy is still challenging in the future.

**Acknowledgements** This work is sponsored by the National Natural Science Foundation of China (Grant Number 52202445, 11602112)

**Author contribution** Qinghua Liu contributed to: conceptualization, methodology, investigation, data curation, writing—original draft, visualization. Qiyu Li: resources, writing—review & editing, formal analysis. Dong Jiang: conceptualization, resources, writing—review & editing, funding acquisition.

**Availability of data and material** These data are collected by the experiment.

**Code availability** The code is written according to the proposed model.

## Declarations

**Conflict of interest** The authors declare that they have no known competing financial interests or personal relationships that could have influenced the work reported in this paper.

## References

- Vakakis AF, Gendelman OV, Bergman LA, Mojahed A, Gzal M (2022) Nonlinear targeted energy transfer: state of the art and new perspectives. *Nonlinear Dyn* 108(2):1–31
- Ding H, Chen LQ (2020) Designs, analysis, and applications of nonlinear energy sinks. *Nonlinear Dyn* 100(4):3061–3107
- Wang J, Zheng Y, Ma Y, Wang B (2024) Experimental study on asymmetric and bistable nonlinear energy sinks enabled by side tracks. *Mech Syst Signal Process* 206:110874
- Zeng Y, Ding H, Du RH, Chen LQ (2022) Micro-amplitude vibration suppression of a bistable nonlinear energy sink constructed by a buckling beam. *Nonlinear Dyn* 108(4):3185–3207
- Romeo F, Sigalov G, Bergman LA, Vakakis AF (2015) Dynamics of a linear oscillator coupled to a bistable light attachment: numerical study. *J Comput Nonlin Dyn* 10(1):011007
- Liu QH, Zhao ZY, Zhang Y, Wang J, Cao JY (2022) Physics-informed sparse identification of bistable structures. *J Phys D: Appl Phys* 56(4):044005
- Liu QH, Hou ZH, Zhang Y, Jing JX, Kerschen G, Cao JY (2022) Nonlinear restoring force identification of strongly nonlinear structures by displacement measurement. *J Vib Acoust* 144(3):031002
- Feldman M (2012) Nonparametric identification of asymmetric nonlinear vibration systems with the Hilbert transform. *J Sound Vib* 331(14):3386–3396
- Braun S, Feldman M (2011) Decomposition of non-stationary signals into varying time scales some aspects of the EMD and HVD methods. *Mech Syst Signal Process* 25(7):2608–2630
- Anastasio D, Fasana A, Garibaldi L, Marchesiello S (2020) Nonlinear dynamics of a duffing-like negative stiffness oscillator: modeling and experimental characterization. *Shock Vib* 2020:3593018
- Anastasio D, Marchesiello S (2020) Experimental characterization of friction in a negative stiffness nonlinear oscillator. *Vibration* 3(2):132–148
- Liu QH, Cao JY, Hu FY, Li D, Hou ZH (2021) Parameter identification of nonlinear bistable piezoelectric structures by two-stage subspace method. *Nonlinear Dyn* 105:2157–2172
- Zhu R, Fei QG, Jiang D, Anastasio D, Marchesiello S (2022) Bayesian model selection in nonlinear subspace identification. *AIAA J* 60(1):92–101
- Wang X, Geng X-F, Mao X-Y, Ding H, Jing X-J, Chen L-Q (2022) Theoretical and experimental analysis of vibration reduction for piecewise linear system by nonlinear energy sink. *Mech Syst Signal Process* 172:109001
- Lund A, Dyke SJ, Song W, Bilonis I (2020) Identification of an experimental nonlinear energy sink device using the unscented Kalman filter. *Mech Syst Signal Process* 136:106512
- Moore KJ (2019) Characteristic nonlinear system identification: a data-driven approach for local nonlinear attachments. *Mech Syst Signal Process* 131:335–347
- Brunton SL, Proctor JL, Kutz JN (2016) Discovering governing equations from data by sparse identification of nonlinear dynamical systems. *Proc Natl Acad Sci USA* 113:3932–3937
- Cheng C, Zhao B, Fu C, Peng ZK, Meng G (2022) A two-stage sparse algorithm for localization and characterization of local nonlinear structures. *J Sound Vib* 526:116823
- Lai Z, Nagarajaiah S (2019) Sparse structural system identification method for nonlinear dynamic systems with hysteresis/inelastic behavior. *Mech Syst Signal Process* 117:813–842
- Liu QH, Cao JY, Zhang Y, Zhao ZY, Kerschen G, Jing XJ (2023) Interpretable sparse identification of a bistable nonlinear energy sink. *Mech Syst Signal Process* 193:110254
- Kaheman K, Kutz JN, Brunton SL (2020) SINDy-PI: a robust algorithm for parallel implicit sparse identification of nonlinear dynamics. *P R Soc Edinb A* 476(2242):20200279

22. Chartrand R (2011) Numerical differentiation of noisy, nonsmooth data. *Int Sch Res Not* 2011:244–248
23. Lin MM, Cheng CM, Peng ZL, Dong XJ, Qu YG, Meng G (2021) Nonlinear dynamical system identification using the sparse regression and separable least squares methods. *J Sound Vib* 505:116141
24. Zhao SY, Cheng CM, Zhang GZ, Lin MM, Peng ZK, Meng G (2023) A nonlinearity-sensitive approach for early damages detection using NOFRFs and the hybrid-LSTM Model. *IEEE Tinstrum Meas.* <https://doi.org/10.1109/TIM.2023.3312473>
25. Hastie T, Tibshirani R, Friedman JH (2009) *The elements of statistical learning: data mining, inference, and prediction*, vol 11. Springer, New York, pp 150–151
26. Qiu D, Li T, Seguy S, Paredes M (2018) Efficient targeted energy transfer of bistable nonlinear energy sink: application to optimal design. *Nonlinear Dyn* 92:443–461
27. Habib G, Romeo F (2017) The tuned bistable nonlinear energy sink. *Nonlinear Dyn* 89(1):179–196
28. Li S, Zhou X, Chen J (2023) Hamiltonian dynamics and targeted energy transfer of a grounded bistable nonlinear energy sink. *Commun Nonlinear Sci* 117:106898
29. Liao X, Chen L, Lee HP (2024) A customizable cam-typed bistable nonlinear energy sink. *Int J Mech Sci* 271:109305
30. Wu Z, Seguy S, Paredes M (2022) Estimation of energy pumping time in bistable nonlinear energy sink and experimental validation. *J Vib Acoust* 144(5):051004
31. Wang J, Zhang C, Li H, Liu Z (2021) Experimental and numerical studies of a novel track bistable nonlinear energy sink with improved energy robustness for structural response mitigation. *Eng Struct* 237:112184
32. Fang ST, Chen KY, Xing JT, Zhou SX, Liao WH (2021) Tuned bistable nonlinear energy sink for simultaneously improved vibration suppression and energy harvesting. *Int J Mech Sci* 212:106838
33. Li HQ, Li A, Kong XR (2021) Design criteria of bistable nonlinear energy sink in steady-state dynamics of beams and plates. *Nonlinear Dyn* 103(2):1475–1497
34. Wang X, Mao XY, Ding H, Lai SK, Chen LQ (2023) Multi-resonance inhibition of a two-degree-of-freedom piecewise system by one nonlinear energy sink. *Int J Dyn Control* 2023:1–19

Springer Nature or its licensor (e.g. a society or other partner) holds exclusive rights to this article under a publishing agreement with the author(s) or other rightsholder(s); author self-archiving of the accepted manuscript version of this article is solely governed by the terms of such publishing agreement and applicable law.